The COVID-19 Anthropause and Its Hydrochemical Impacts: A Case Study of Chonburi Coast, Thailand

Chakhrti Ruengsorn[1*], Shettapong Meksumpun[1], Sataporn Rattanapreechachan[1], Amolvan Aumngamsup[1] and Poratape Jendanklang[2]

ABSTRACT

This study investigates the impact of COVID-19 lockdown measures on coastal ecosystems in Chonburi Province, Thailand. A comparative analysis of water and sediment quality parameters from 10 sampling stations was conducted between the pre-pandemic (2017–2019) and pandemic (2020–2021) periods. The lockdown period showed statistically significant improvements ($p<0.05$) across multiple water quality parameters: a 27% increase in transparency, a 29% reduction in total suspended solids, and a 42% decrease in PO_4^{3-}-P concentrations in surface water. Concurrently, bottom water showed reductions of 51% and 43% in NO_2^-+NO_3^--N and PO_4^{3-}-P levels, respectively. Sedimentary parameters similarly improved, showing reductions of 10%, 23%, and 9% in AVS, $Si(OH)_4$-Si, and PO_4^{3-}-P. Counterintuitively, phytoplankton biomass (Chl *a*) increased dramatically (101–116%), which is attributable to improved light availability (27% higher transparency) and substantial nutrient fluxes from sediments, where NH_4^+-N and PO_4^{3-}-P concentrations exceeded bottom water levels by 90- and 213-fold, respectively. Spatial analysis revealed stronger fluvial influences near river mouths compared to distal areas. The 84% reduction in tourist numbers significantly decreased nutrient inputs ($p<0.05$; based on the pre-lockdown correlation), though persistent N:P imbalances (surface 17:1, bottom 29:1) and sedimentary nutrient reservoirs maintained eutrophic conditions. These findings demonstrate the rapid responsiveness of coastal ecosystems to reduced anthropogenic pressure. They further underscore the critical need for implementing targeted sediment management strategies in areas with high land-based runoff to achieve sustainable water quality improvements.

Keywords: Chonburi Province, COVID-19 pandemic, Mitigation, Sediment quality, Thailand, Water quality

INTRODUCTION

The Coronavirus Disease 2019 (COVID-19) pandemic has been recognized as one of the most significant global challenges since World War II (Gautam, 2020). Following the World Health Organization's (WHO) declaration of COVID-19 as a Public Health Emergency of International Concern (PHEIC) on January 30, 2020 (World Health Organization, 2020a; 2020b), Thailand implemented a nationwide lockdown in mid-March 2020 (Ministry of Public Health, 2021), which caused the average number of tourists in Chonburi Province to plummet from1.207±0.145 million per month (2017–2019) to just 0.188±0.255 million per month (2020–2021) (Ministry of Tourism and Sports, 2025). These measures were designed to control pandemic spread, reduce transmission rates, and decrease virus-related mortality (Cherif *et al*., 2020). While these restrictions disrupted various

[1]Department of Marine Science, Faculty of Fisheries, Kasetsart University, Bangkok, Thailand
[2]Department of Fisheries, Rayong Marine Fisheries Research and Development Center, Rayong, Thailand
*Corresponding author. E-mail address: ffiscrr@ku.ac.th
Received 4 August 2025 / Accepted 30 December 2025

human activities including transportation, industry, and tourism, they simultaneously yielded unexpected environmental benefits by reducing anthropogenic pressures on ecosystems (Lal *et al*., 2020; Zhu *et al*., 2020; Mishra *et al*., 2024).

Global environmental change, primarily driven by human activities, poses a significant threat to sustainability. While the COVID-19 pandemic lockdowns had substantial health and economic consequences, their impact on environmental health has emerged as an important area of scientific inquiry (Loh *et al*., 2022). Studies worldwide have reported improvements in water quality indices during lockdown periods, which subsequently enhanced ecosystem recovery processes for various aquatic species including fish, sea turtles, marine mammals, and aquatic birds. Furthermore, ecologically sensitive habitats such as mangroves and coral reefs showed signs of rejuvenation during pandemic-related restrictions (Mallik *et al*., 2022). Notable water quality improvements during lockdowns included an increase in dissolved oxygen (DO) of 19.5–25.3% in China, India and Turkey, and decreases in ammonium-nitrogen (NH_4^+-N) in China and nitrate-nitrogen (NO_3^--N) in India of 31.5% and 56.0%, respectively (Chakraborty *et al*., 2020; Tokatlı and Varol, 2021; Xu *et al*., 2021). Water transparency in Bohai Bay, China, also increased by 52.4% during 2020–2022 compared with 2017–2019, attributed to restrictions on urban transportation (Yan *et al*., 2025). In Thailand, total nitrogen (TN), total phosphorus (TP), and biochemical oxygen demand (BOD) in surface waters at Ko Yo, Songkhla, were significantly higher before the COVID-19 crisis than during the pandemic (Sinutok *et al*., 2021). Despite documented improvements, comprehensive studies on the pandemic's impacts on both the water column and sediment quality in coastal Thailand remain limited, creating a critical knowledge gap in understanding the full environmental consequences of COVID-19 restrictions.

To address this critical knowledge gap, our study systematically quantified and compared water and sediment quality parameters during two distinct periods: pre-COVID-19 (2017–2019) and during-COVID-19 (2020–2021). We hypothesized that reduced anthropogenic pressures during the pandemic period significantly improved coastal water and sediment conditions in Chonburi Province, Thailand.

MATERIALS AND METHODS

The study site is located in Chonburi Province, a coastal area in the eastern upper Gulf of Thailand (Figure 1). The province's topography comprises five terrain types: rolling plains and hills, coastal plains, the Bang Pakong River basin, steep mountainous areas, and numerous small islands. The coastal plain stretches from the Bang Pakong River mouth to Sattahip District, forming a narrow strip interspersed with small coastal mountains. The Bang Pakong River basin includes the Khlong Luang Canal, a 130-km-long waterway that originates in Bo Thong and Ban Bueng Districts, flows through Phanat Nikhom, merges with Khlong Phan Thong, and eventually drains into the Bang Pakong River. The river's alluvial deposits have created fertile lowlands ideal for agriculture. Chonburi Province is a core zone of Thailand's Eastern Seaboard industrial development plan, home to Laem Chabang Deep Sea Port and industrial estates (Laem Chabang, Bowin, and Bang Pakong). It also boasts popular tourist destinations such as Bangsaen Beach and Pattaya Beach (Department of Marine and Coastal Resources, 2018). Previous studies indicate that during the flood season (July), runoff into the inner Gulf of Thailand is most pronounced near the estuaries of the Chao Phraya and Bang Pakong Rivers. Salinity gradients extend approximately 25 km seaward from the Chao Phraya estuary. In the mid-flood season (July), salinity near the Bang Pakong and Chao Phraya river mouths fluctuates significantly over a wide area (Faculty of Fisheries, 2018).

This study was conducted over 13 sampling events between April 2017 and August 2021 (Table 1) to capture representative low- and high-flow periods, corresponding to Thailand's southwest (SW) and northeast (NE) monsoon periods (TMD, 2016). These periods also serve as proxies for the pre- and during-COVID-19 pandemic eras. Data analysis aligned with Thailand's nationwide

lockdown announcement in mid-March 2020 (Ministry of Public Health, 2021). The study period was divided into two datasets: 2017–2019 (pre-pandemic) and 2020–2021 (during-pandemic). Field surveys were conducted at 10 coastal stations in Chonburi Province during each sampling period (Figure 1; Stations CH1–CH10). These stations covered the study area from the northern Bang Pakong River estuary (CH1) to the southern coastal zone of Sattahip District (CH10).

Table 1. Spatial and temporal design of the study: sampling station locations and sampling periods along the eastern coast of the upper Gulf of Thailand in Chonburi Province.

Station	Position (UTM, 47P)		Study periods	
	E	N	Pre-COVID-19	During-COVID-19
CH1	702978	1482971	April, July, December 2017, April, July 2018, and September, December 2019	May, August, November 2020, February, May, and August 2021
CH2	703236	1470962		
CH3	696353	1461870		
CH4	707280	1457559		
CH5	702930	1442275		
CH6	697903	1439187		
CH7	690762	1419103		
CH8	703947	1416657		
CH9	692990	1409569		
CH10	695566	1400950		

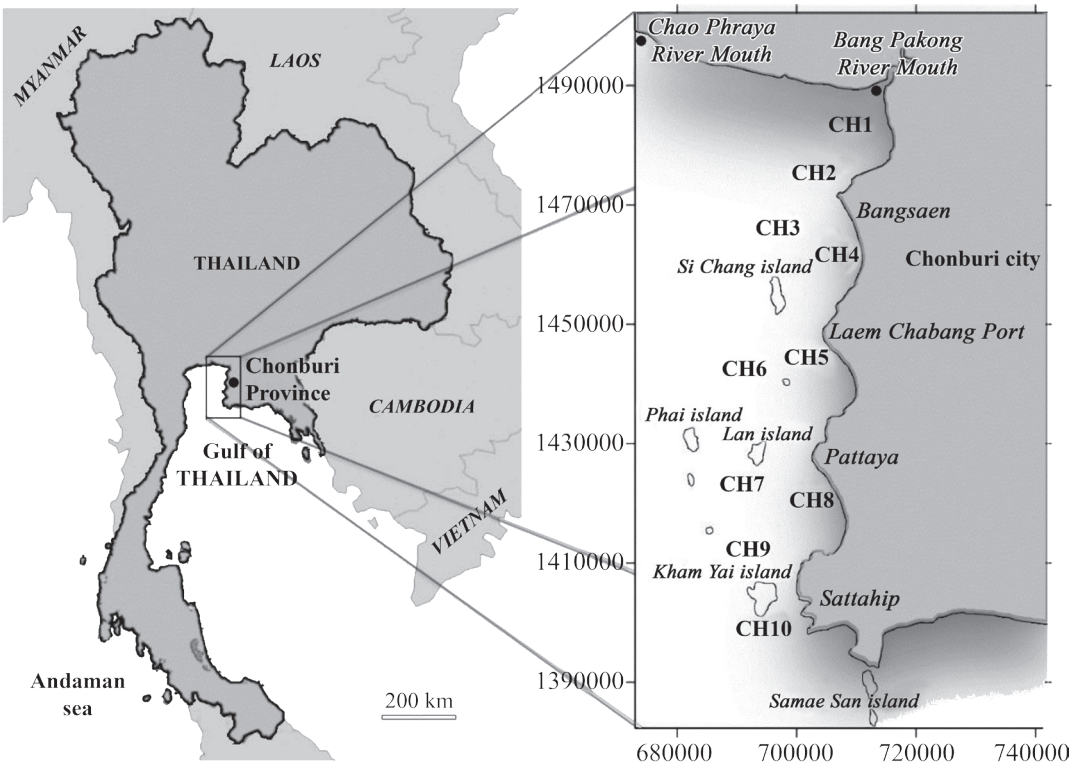

Figure 1. Sampling stations along the eastern coast of the upper Gulf of Thailand in Chonburi Province.

Water measurements and analysis

Water quality was measured in situ and water samples were collected from both the surface and bottom water columns at each coastal station. Water transparency was determined using a Secchi disk. Temperature, salinity, and dissolved oxygen (DO) were measured in situ using a YSI Professional Plus Multiparameter instrument (YSI Incorporated, USA).

Water samples for chlorophyll a (Chl *a*), total suspended solids (TSS), and nutrient analysis were collected using a Kemmerer Water Sampler (Wildlife Supply Company, USA). Samples for Chl *a* and TSS were stored in light-protected polyethylene bags and filtered through pre-weighed Whatman GF/F (for Chl *a*) and GF/C (for TSS) filters using standard Millipore filtration. Chl *a* was analyzed using a spectrophotometric method, while TSS was determined using the particulate material analysis method (Parsons *et al*., 1984).

For nutrient analysis (NH_4^+-N, NO_2^-+ NO_3^--N, $Si(OH)_4$-Si, PO_4^{3-}-P), water samples were filtered onboard through GF/F filters and analyzed using a Bran+Luebbe Auto-analyzer, TRAACS 2000 Continuous-Flow model.

Furthermore, we assessed land-derived influences on coastal water quality during contrasting hydrological regimes —low-flow (dry season) and high-flow (monsoon season) —to quantify runoff-mediated anthropogenic impacts in Chonburi Province. This analysis used official 2017–2021 runoff statistics from the Chao Phraya and Bang Pakong Rivers, as reported by the Eastern Regional Irrigation Hydrology Center (2023).

Sediment sampling and analysis

Undisturbed sediment cores were collected by SCUBA divers using an acrylic corer sampler (9.5 cm diameter × 50.0 cm height). The top 0–1 cm layer was subsampled and stored at -20 °C for analysis of acid volatile sulfides (AVS), organic matter (OM), fine grain size (FGS; particle size <63 μm), and pore-water nutrients.

AVS was measured using Gastech detector tubes (Allen *et al*., 1993; Gastec Corporation, 2023). OM was analyzed via the loss on ignition (LOI) method (Dean, 1974; Bengtsson and Enell, 1986; Verardo *et al*., 1990; Virkanen *et al*., 1997). FGS was determined by the sieving method (ASTM, 2017). Pore-water nutrients (NH_4^+-N, NO_2^-+NO_3^--N, $Si(OH)_4$-Si, PO_4^{3-}-P) were analyzed using the same methods as for the water samples.

Data analysis

Water and sediment quality data were analyzed using standard statistical procedures. Normality was assessed with the Shapiro–Wilk test (Shapiro and Wilk, 1965) and homoscedasticity with the Breusch–Pagan test (Breusch and Pagan, 1979). When data violated parametric assumptions (non-normal distributions or unequal variances), the Mann-Whitney U test was used as a non-parametric alternative for comparing independent samples across periods. Statistical associations were assessed using either linear regression (coefficient of determination, r^2) (Kutner *et al*., 2005) or Spearman's rank correlation coefficient (ρ), depending on data distribution and the interpretative purpose of the analysis. Results are presented as the r^2 value for regressions and the correlation coefficient (ρ) with its corresponding p-value for correlations, respectively. Statistical significance for Spearman's rank correlation was set at $p<0.05$. Statistical analyses were conducted using IBM SPSS (version 28) or other suitable statistical software. Descriptive statistics (mean±SD) were also used to characterize baseline conditions and to illustrate differences between the pre- and during-COVID-19 pandemic periods, with spatiotemporal variations presented graphically where appropriate.

RESULTS AND DISCUSSION

Seasonal variation and runoff impacts

Thailand's three-season climate—summer (mid-February to mid-May), rainy season (mid-May to late October), and winter (mid-October to mid-February) (Meteorological Information Office, 2019)—fundamentally influenced coastal

hydrodynamics in our study area. Bathymetric surveys revealed seafloor depths ranging from 4.5 m (station CH1) to 24.2 m (CH6), which may contribute to spatial thermal variability as evidenced by large standard deviations, particularly during winter months. Mean (±SD) temperatures, averaged across stations CH1–CH10, showed typical seasonal patterns: surface waters averaged 31.1±0.5 °C (summer), 30.1±0.6 °C (rainy), and 28.1±1.1 °C (winter), while bottom waters averaged 30.8±0.5 °C, 29.7±0.4 °C, and 27.7±1.1 °C, respectively (Figure 2a).

Hydrological data from the Eastern Regional Irrigation Hydrology Center (2023) revealed clear discharge contrasts between low-flow (December–May) and high-flow (June–November) periods. The Chao Phraya River showed monthly averages of 522.02±67.18 – 625.42±121.09 million m³ (low-flow) versus 536.95±286.88 – 1,419.90± 1,070.00 million m³ (high-flow), while the Bang Pakong River discharged 75.83±30.84 – 104.98± 82.80 million m³ versus 128.86±135.04 – 997.37± 410.57 million m³, respectively. These discharge differentials may have contributed to salinity variation, with mean (±SD) salinity averaged across CH1–CH10 appearing higher during the low-flow period than during the high-flow period in both layers (Figure 2b): 31.9±0.9 vs 29.2±5.0 psu at the surface, and 32.0±0.7 vs 30.2±4.1 psu at the bottom.

Figures 3 to 5 clearly demonstrate that the spatial distributions of water and sediment quality parameters exhibit declining gradients from peak values near the river mouth (CH1) toward lower concentrations in the coastal area of Sattahip District (CH10). This trend is consistent across most parameters, except for PO_4^{3-}-P in bottom water and sediment, which showed distinct spatial variability. Similarly, transparency measurements support these observations, with seawater clarity increasing progressively at stations farther from the river mouth. Station-specific analysis indicated generally higher parameter values in the near-river mouth group (CH1–CH5) compared to the far river-mouth group (CH6–CH10), indicating stronger fluvial influence on coastal water quality in Chonburi Province near the river mouth.

An exception was observed at Station CH8 near Jomtien Beach (located in South Pattaya, Bang Lamung District), which is characterized by a narrow sandy shore (~20 m wide) and intensive anthropogenic activities (tourism, residential areas, and fishing/tourist boat piers). This site exhibited anomalous transparency, TSS, and sediment quality parameters, deviating from the trends within the far river-mouth group.

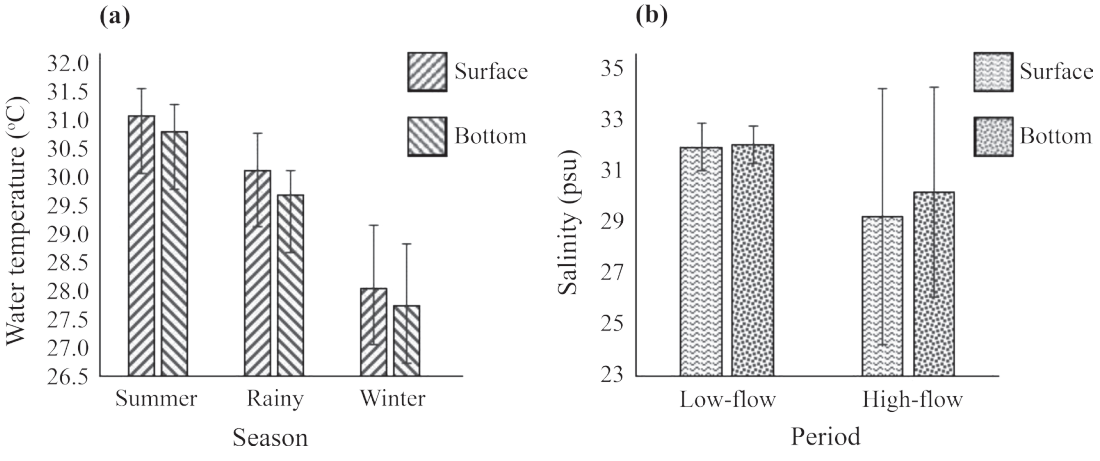

Figure 2. Mean (±SD) (a) water temperature by season and (b) salinity by hydrodynamic period (low-flow vs. high-flow) in surface and bottom layers, averaged across stations CH1–CH10 during the study period.

The hydrological regimes distinctly influenced the two station groups (Table 2). For near-river mouth stations (CH1–CH5), the high-flow period (June–November) exerted the strongest statistical effects, particularly on surface and bottom water quality. Surface water parameters showed significant negative correlations with salinity and $Si(OH)_4$-Si, while Chl *a* exhibited a strong positive correlation. Bottom water responses were similarly pronounced, with significant correlations in salinity, Chl *a*, and dissolved oxygen. In contrast, sediment parameters showed no significant correlations with discharge.

For stations farther from the river mouth (CH6–CH10), significant correlations were also observed during the high-flow period, but the strength

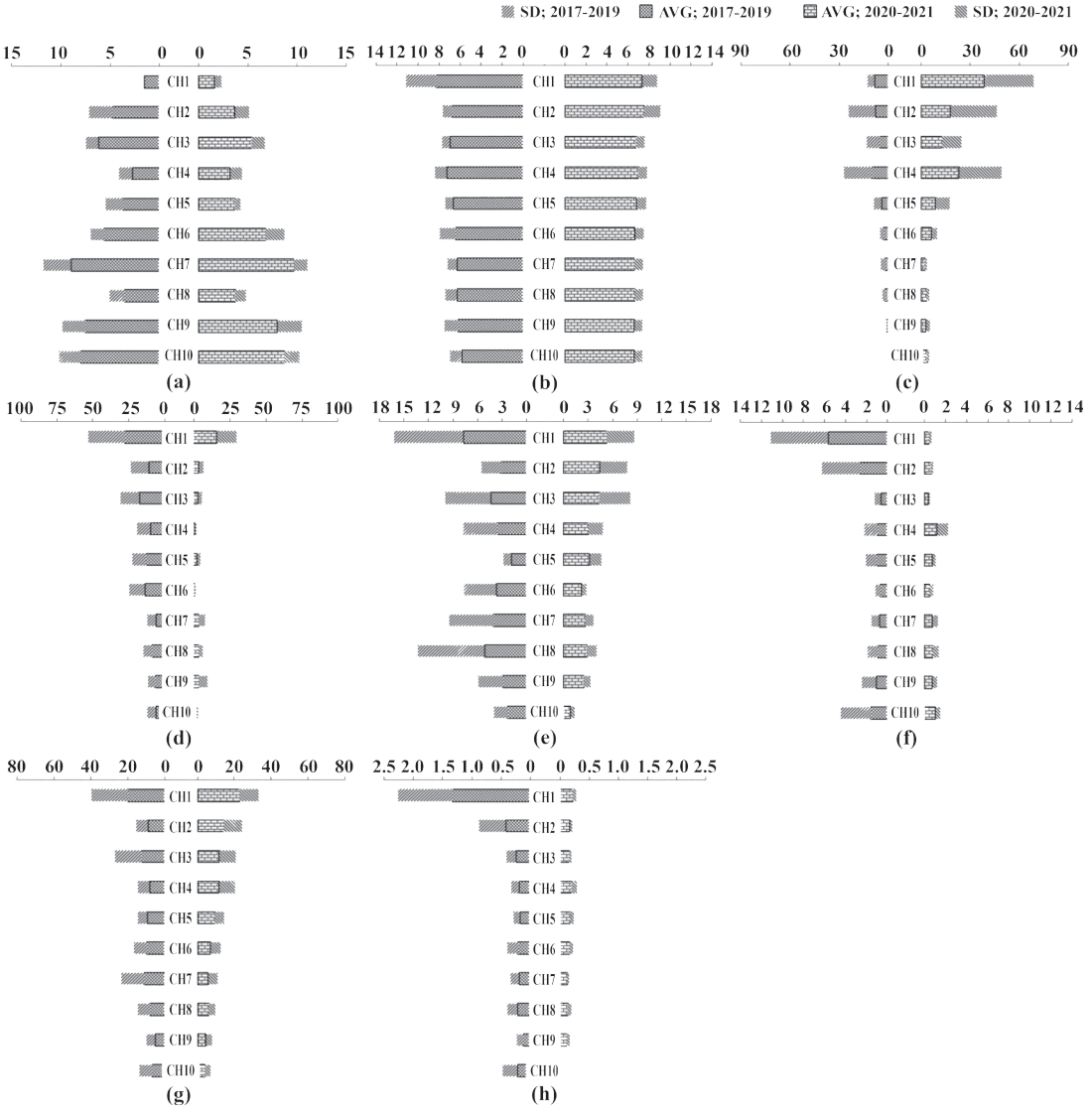

Figure 3. Spatial distribution patterns and average values (AVG and SD) of surface-water quality parameters at stations CH1−CH10, shown as pre-pandemic (2017–2019; left) and during-pandemic (2020–2021; right) periods: (a) transparency (m), (b) DO ($mg \cdot L^{-1}$), (c) Chl *a* ($\mu g \cdot L^{-1}$), (d) TSS ($mg \cdot L^{-1}$), (e) NH_4^+-N (μM), (f) NO_2^-+NO_3^--N (μM), (g) $Si(OH)_4$-Si (μM), and (h) PO_4^{3-}-P (μM).

and pattern of responses differed slightly. Bottom water showed the strongest responses, particularly in salinity and Chl *a*. Surface water correlations were slightly weaker but still significant for salinity and Chl *a*. As with the near-river group, sediment parameters showed no significant relationships with discharge. Overall, both station groups were more responsive to hydrological changes during the high-flow season, with no significant correlations found during the low-flow period. These results highlight that seasonal discharge variations have a stronger influence on water quality parameters than on sediment characteristics, regardless of proximity to the river mouth, though the relative strength of responses differs between surface and bottom waters across the two zones.

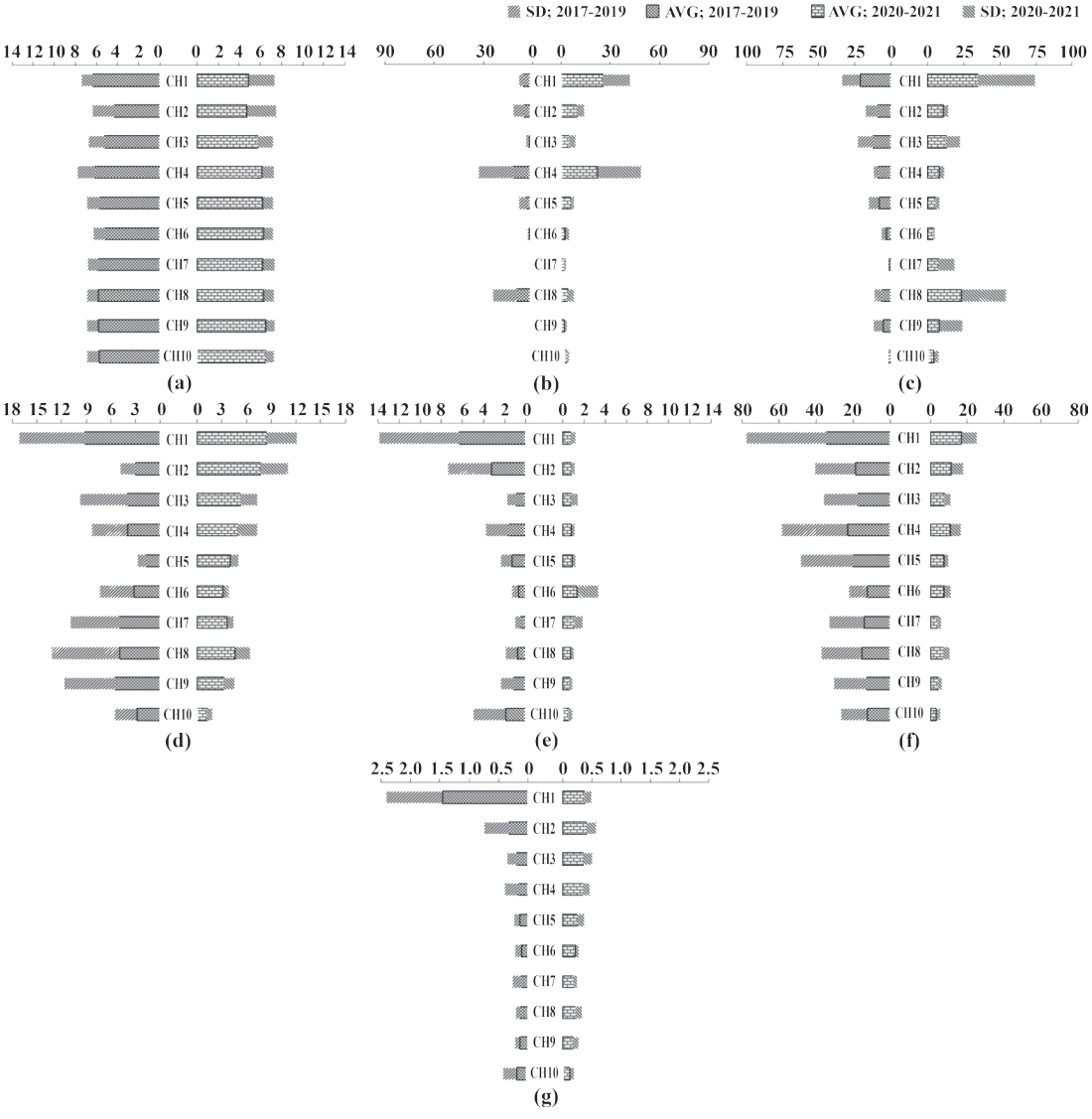

Figure 4. Spatial distribution patterns and average values (AVG and SD) of bottom-water quality parameters at stations HH1-CH10, shown as pre-pandemic (2017–2019; left) and during-pandemic (2020–2021; right) periods: (a) DO ($mg \cdot L^{-1}$), (b) Chl *a* ($\mu g \cdot L^{-1}$), (c) TSS ($mg \cdot L^{-1}$), (d) NH4+-N (μM), (e) NO_2^-+NO_3^--N (μM), (f) $Si(OH)_4$-Si (μM), and (g) PO_4^{3-}-P (μM).

Doney *et al*. (2009), Seitzinger *et al*. (2010), and Bianchi *et al*. (2013) provide comprehensive insights into how human activities degrade water and sediment quality in estuarine and coastal ecosystems through land-based runoff. Runoff volume can reduce water transparency due to elevated TSS from urban and agricultural runoff, increase nutrient concentrations (ammonium, nitrite, nitrate, silicate, and phosphate) from wastewater discharge, fertilizers, and industrial effluents, leading to eutrophication and harmful algal blooms, increase AVS in organically enriched sediments, indicating hypoxic/anoxic conditions, accumulated fine-grained sediments and organic matter due to enhanced particle deposition from runoff, and enhance sediment nutrient retention

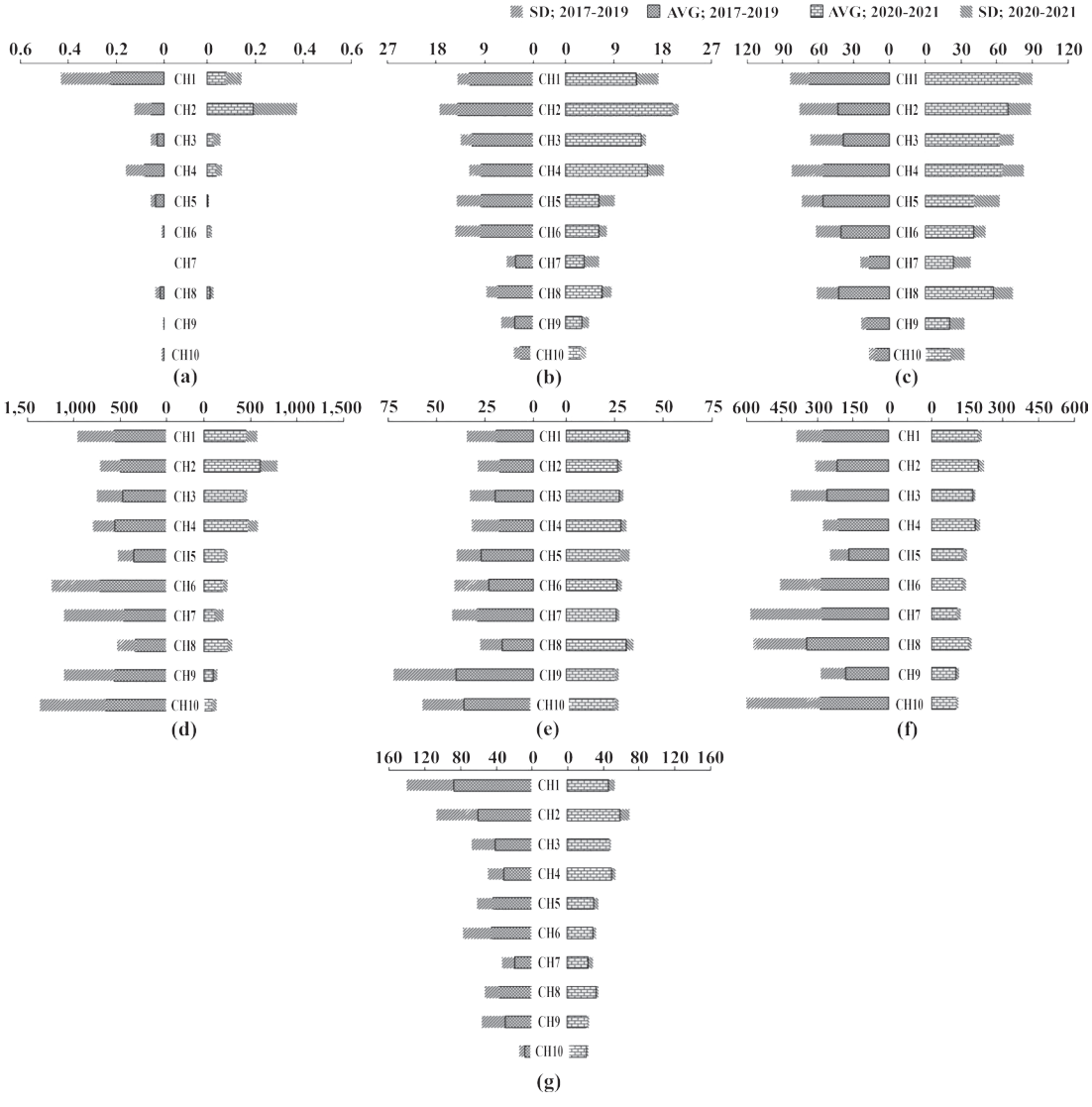

Figure 5. Spatial distribution patterns and average values (AVG and SD) of sediment quality in 0–1 cm depth layer at stations CH1-CH10, shown as pre-pandemic (2017–2019; left) and during-pandemic (2020–2021; right) periods: (a) AVS ($mg \cdot g^{-1}$), (b) OM (%), (c) FGS (%), (d) NH_4^+-N (μM), (e) NO_2^-+NO_3^--N (μM), (f) $Si(OH)_4$-Si (μM), and (g) PO_4^{3-}-P (μM).

Table 2. Summary of correlation between hydrological regimes and environmental parameters for each station group.

Station group	Key findings	Dominant flow period	Statistical strength	Significant parameters (ρ, p-value)
CH1–CH5 (Near-river mouth)	Strong correlation with hydrological regimes, especially in high-flow period.	High-flow (Jun–Nov)	Surface water> Bottom water > Sediment	Surface water: • Salinity: ρ = -0.853, p<0.001 • Chl *a*: ρ = 0.714, p = 0.011 • $Si(OH)_4$-Si: ρ = -0.740, p = 0.004
				Bottom water: • Salinity: ρ = -0.804, p = 0.002 • Chl *a*: ρ = 0.750, p = 0.004 • $Si(OH)_4$-Si: ρ = -0.704, p = 0.011
				Sediment: No significant correlations found.
CH6–CH10 (Far from river mouth)	Moderate correlation, fewer significant parameters	High-flow (Jun–Nov)	Bottom water> Surface water> Sediment	Surface water: • Salinity: ρ = -0.804, p = 0.002 • Chl *a*: ρ = 0.705, p = 0.015 • $Si(OH)_4$-Si: ρ = -0.603, p = 0.038
				Bottom water: • Salinity: ρ = -0.853, p<0.001 • Chl *a*: ρ = 0.804, p = 0.002 • $Si(OH)_4$-Si: ρ = -0.750, p = 0.004
				Sediment: No significant correlations found.

Note: * Significant (p<0.05); ** Highly significant (p<0.01); Mann-Whitney U Test.; Statistical strength: Ordered by ρ.

and potential release (NH_4^+, NO_2^-, NO_3^-, silicate, PO_4^{3-}), where sediments act as a nutrient reservoir and can release these compounds back into the water column under certain conditions. These studies collectively emphasize that land-based pollution significantly alters coastal ecosystems, with long-term consequences for biogeochemical cycles.

Furthermore, our analysis of standard deviations (SD) in environmental quality parameters reveals lower variability during the during-pandemic period (2020–2021) compared to the pre-pandemic period (2017–2019) (Figures 3–5). This trend is consistent across most water and sediment quality metrics, with the notable exceptions of DO and Chl *a*. The observed reduction in SD values suggests that lockdown measures enabled coastal ecosystems to revert to more natural seasonal patterns, likely due to diminished anthropogenic disturbances. These findings align with Zambrano-Monserrate *et al*. (2020), who reported the lack of tourists, as a result of the social distancing measures due to the new coronavirus pandemic, has caused a notable change in the appearance of many coasts worldwide.

The estuaries serve dual roles as both sources and sinks for land-derived pollutants, with lockdown data demonstrating the pronounced sensitivity of external pollutant inputs to anthropogenic activity restrictions. Notably, localized pollution sources - particularly from Chonburi's Laem Chabang Industrial Estate, fisheries operations, residential discharges, and especially tourism-related activities - remain critical factors requiring comprehensive evaluation in water and sediment quality assessments.

Temporal variations between the pre- and during-COVID-19 pandemic periods

The statistical analysis revealed significant water quality improvements during COVID-19 lockdowns across Chonburi's coastal ecosystems (Table 3). Surface waters exhibited a 27% increase in transparency ($p<0.05$), coupled with a 29% reduction in TSS ($p<0.05$) and a 42% reduction in PO_4^{3-}-P ($p<0.01$), while bottom waters showed even more pronounced decreases in NO_2^-+NO_3^--N (51%, $p<0.05$) and PO_4^{3-}-P (43%, $p<0.01$).

Sediment quality similarly improved with significant reductions in AVS (10%, $p<0.05$), $Si(OH)_4$-Si (23%, $p<0.05$), and PO_4^{3-}-P (9%, $p<0.01$). Paradoxically, phytoplankton biomass (Chl *a*) surged dramatically in both surface (101%, $p<0.01$) and bottom waters (116%, $p<0.01$), likely fueled by enhanced light availability (higher transparency) and nutrient fluxes from sediments, where sediment pore-water NH_4^+-N and PO_4^{3-}-P concentrations remained orders of magnitude higher than in the water column. These findings collectively demonstrate that reduced anthropogenic pressures during lockdowns rapidly improved multiple water quality indicators, though legacy effects in sediments and altered nutrient cycling stimulated phytoplankton productivity despite overall water quality enhancements.

Table 3. Comparison of water and sediment quality parameters (stations CH1-CH10) between the pre- COVID-19 (2017–2019) and during-COVID-19 (2020–2021) periods (mean±SD), with the percentage change and Mann–Whitney U test *p*-values.

Environmental quality	Parameter (Unit)	Value or concentration (average ±SD)		Change		p-value
		Pre-COVID-19	During-COVID-19	Trend	(%)	
Surface water	Transparency (m)	4.12±2.45	5.23±2.89	↑	27	0.032
	DO ($mg \cdot L^{-1}$)	6.78±1.02	6.91±1.15	↑	2	0.124
	Chl *a* ($\mu g \cdot L^{-1}$)	5.21±8.34	10.45±15.67	↑	101	0.008
	TSS ($mg \cdot L^{-1}$)	12.34±12.56	8.76±9.23	↓	-29	0.045
	NH_4^+-N (µM)	3.56±4.21	3.12±2.89	↓	-12	0.210
	NO_2^-+NO_3^--N (µM)	1.45±2.34	0.89±1.12	↓	-39	0.087
	$Si(OH)_4$-Si (µM)	10.23±9.45	12.56±10.23	↑	23	0.015
	PO_4^{3-}-P (µM)	0.31±0.45	0.18±0.23	↓	-42	0.003
Bottom water	DO ($mg \cdot L^{-1}$)	5.92±1.32	6.01±1.45	↑	2	0.042
	Chl *a* ($\mu g \cdot L^{-1}$)	4.56±7.89	9.87±12.45	↑	116	0.006
	TSS ($mg \cdot L^{-1}$)	8.23±9.12	10.45±15.67	↑	27	0.128
	NH_4^+-N (µM)	4.21±5.34	4.56±3.89	↑	8	0.087
	NO_2^-+NO_3^--N (µM)	1.89±3.45	0.92±1.23	↓	-51	0.015
	$Si(OH)_4$-Si (µM)	15.23±18.45	14.56±12.23	↓	-4	0.210
	PO_4^{3-}-P (µM)	0.28±0.42	0.16±0.21	↓	-43	0.003
Sediment (0–1 cm depth)	AVS ($mg \cdot g^{-1}$)	0.042±0.068	0.038±0.052	↓	-10	0.021
	OM (%)	8.12±5.34	10.45±6.89	↑	29	0.003
	FGS (%)	42.15±25.67	53.89±23.45	↑	28	0.045
	NH_4^+-N (µM)	456.78±423.56	412.34±287.23	↓	-10	0.210
	NO_2^-+NO_3^--N (µM)	24.56±18.34	28.12±5.67	↑	15	0.087
	$Si(OH)_4$-Si (µM)	218.45±178.23	168.34±45.67	↓	-23	0.015
	PO_4^{3-}-P (µM)	37.29±34.56	34.12±16.78	↓	-9	0.006

Note: Change trending quality: (↑) increase and (↓) decrease.

Regression analysis of nutrient relationships between sediment and bottom water during pre-COVID-19 (n = 70) and during-COVID-19 (n = 60) periods (Figure 6) revealed that NH_4^+-N and PO_4^{3-}-P concentrations in bottom water exhibited increasing trends corresponding to sediment concentrations, particularly during the COVID-19 period. The sediment contained substantially higher nutrient levels—approximately 90 times greater for NH_4^+-N and 213 times greater for PO_4^{3-}-P—compared to bottom water, creating strong concentration gradients that may have driven nutrient flux from sediment to the water column through advection, diffusive flux, and bioturbation processes (Regnier *et al*., 2013). This transport mechanism may partly explain the observed decreases in sediment PO_4^{3-}-P during the COVID-19 period (Table 3), whereas sediment NH_4^+-N decreased only slightly and was not statistically significant.

During the COVID-19 period, while the flux of NH_4^+-N and PO_4^{3-}-P from sediment to bottom water was likely reduced and did not result in substantial accumulation of these nutrients in the bottom water column (NH_4^+-N showed only a

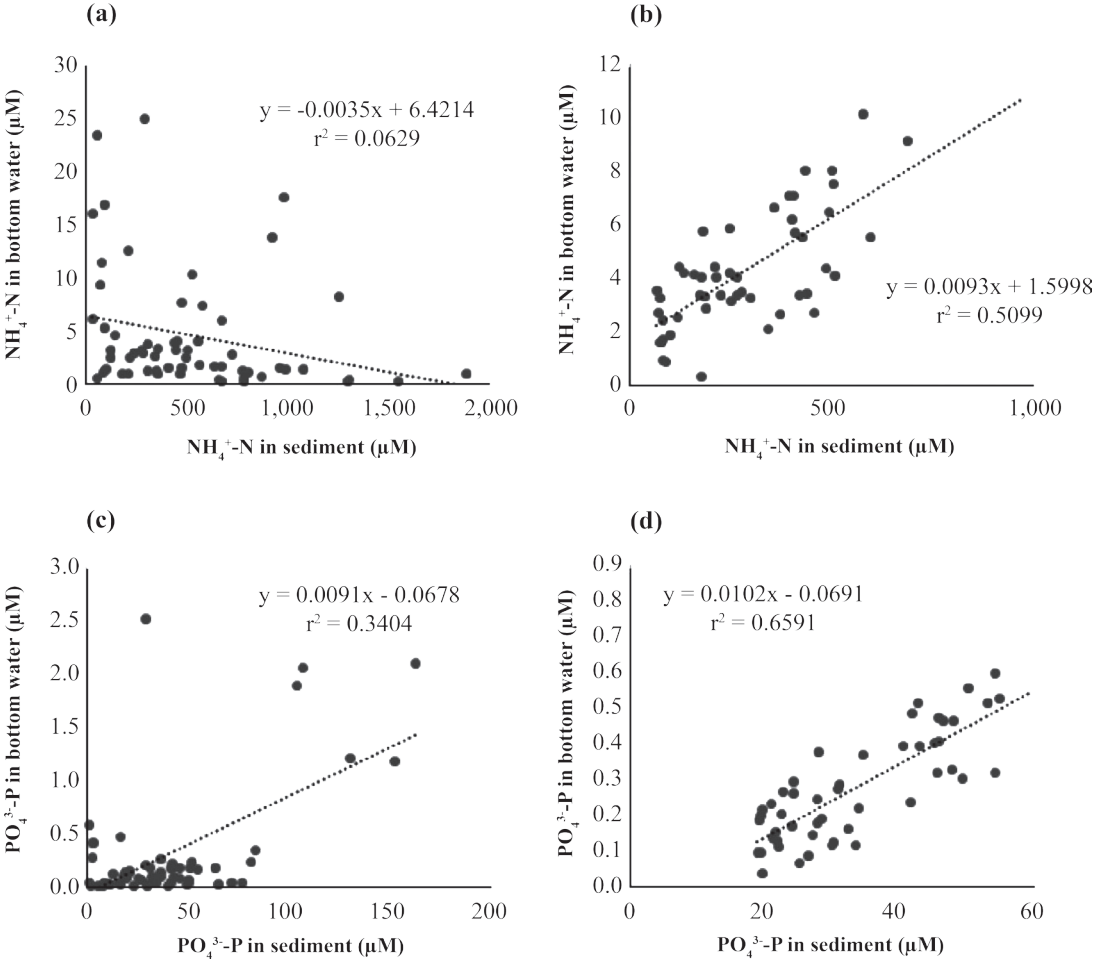

Figure 6. Linear regression relationships between nutrient concentrations in sediment and bottom water (µM) during the pre-COVID-19 period (2017–2019) and during the COVID-19 period (2020–2021): (a) NH_4^+-N (pre-COVID-19), (b) NH_4^+-N (during COVID-19), (c) PO_4^{3-}-P (pre-COVID-19), and (d) PO_4^{3-}-P (during COVID-19). Dotted lines indicate fitted regression lines; the regression equation and R^2 are shown in each panel.

marginal 8% increase, whereas PO_4^{3-}-P decreased by 43%), the dramatic concurrent increases in Chl *a* production (101% in surface water and 116% in bottom water) coupled with enhanced water transparency (27%) (Table 3) strongly suggest that phytoplankton efficiently utilized these nutrients for photosynthesis when both nutrient availability and light conditions became favorable (Meksumpun, 2015). This biological uptake mechanism may help explain the observed reductions of NH_4^+-N and PO_4^{3-}-P in surface water and PO_4^{3-}-P in bottom water, while the slight, statistically insignificant increase in bottom water NH_4^+-N likely reflects continued sediment release that slightly exceeded phytoplankton demand for this nutrient.

Analysis of nutrient ratios during the COVID-19 period based on values in Table 3 reveals distinct N:P dynamics between water layers: surface waters showed an N:P ratio of 17:1, notably lower than the 29:1 ratio in bottom waters. This disparity stems from higher NH_4^+-N concentrations in bottom water (4.56±3.89 µM) compared to surface water (3.12±2.89 µM), reflecting stronger sediment influence (412.34±287.23 µM NH_4^+-N). While these nutrient-rich conditions (particularly in bottom waters) promote phytoplankton growth, the system shows potential phosphorus limitation, as evidenced by slightly lower PO_4^{3-}-P concentrations in bottom water (0.16±0.21 µM) compared to surface water (0.18±0.23 µM). Nevertheless, these PO_4^{3-}-P concentrations remain sufficient to maintain mesotrophic to eutrophic conditions (Ignatiades *et al*., 1992; Dodds and Whiles, 2010; Karydis, 2005), suggesting that bottom waters offer more favorable nutrient conditions for phytoplankton.

While primary production typically dominates in surface waters due to greater light availability for photosynthesis (Meksumpun, 2015), the study area (stations CH1–CH10) exhibited unique characteristics. Transparency values ranged between 1.5–9.0 m (low-flow period) and 1.6–9.6 m (high-flow period), with seafloor depths of 4.5–24.2 m. Calculated euphotic zone depths (using a 1.84:1 ratio of euphotic depth to Secchi disk depth; Borowiak and Borowiak, 2016) spanned 2.3–16.6 m (low-flow period) and 3.4–16.7 m (high-flow period). These conditions allowed sufficient light penetration to reach bottom waters, particularly in coastal areas of Sattahip District (stations CH9 and CH10, except CH6; Figure 7), supporting phytoplankton photosynthesis even near the seafloor. This may help explain the observed increase in Chl *a* concentration during the lockdown period.

The COVID-19 period (2020–2021) brought measurable improvements to coastal water and sediment quality in Chonburi Province, yet persistent challenges were observed through elevated chlorophyll *a* (Chl *a*), organic matter (OM), fine-grained sediment (FGS) accumulation, and sustained nutrient fluxes from sediments. Parallel observations from Japan's Seto Inland Sea demonstrate similar dynamics, where red tide frequency peaked at 299 incidents in 1976 before declining to approximately 100 annual events following implementation of the 1973 Special Measures Law that reduced industrial nutrient loads by 50% (Imai *et al*., 2006). However, residual nutrient levels continue to support algal blooms, illustrating the persistent impacts of eutrophication. Conley *et al*. (2009) further established that sediment nutrient legacy effects can maintain eutrophic conditions for decades after external load reductions, as documented in Baltic Sea ecosystems. These findings collectively indicate that while short-term water quality enhancements are possible, achieving sustainable recovery in Chonburi's coastal waters will require comprehensive sediment management strategies to address long-term nutrient cycling and storage dynamics.

Direct pollution accumulation in Chonburi's coastal areas, apart from riverine runoff, stems from human activities such as operations in the Laem Chabang Industrial Estate and Deep-Sea Port, fisheries, and residential communities. However, the sector most visibly impacted by the COVID-19 pandemic was tourism. Lockdown measures caused the average number of tourists in Chonburi to plummet from 1.207±0.145 million per month (2017–2019) to just 0.188±0.255 million per month (2020–2021) (Ministry of Tourism and Sports, 2025).

This study assessed the potential coastal release of NH_4^+-N and PO_4^{3-}-P specifically from tourist bathing wastewater (excluding other tourism-related graywater), calculated using pre- and during-COVID-19 visitor data. With an average bathing water use of 36.13±8.80 L·person^{-1} and effluent concentrations of 25.25 μM (353.50 μg·L^{-1}) for NH_4^+-N and 24.42 μM (757.02 μg·L^{-1}) for PO_4^{3-}-P (Pollution Control Department, 2005), the net waste discharge averaged 427±51 kg·month^{-1} (NH_4^+-N) and 33±4 kg•month-1 (PO_4^{3-}-P) pre-pandemic, dropping to 66±90 kg·month^{-1} (NH_4^+-N) and 5±7 kg·month^{-1} (PO_4^{3-}-P) during the pandemic—an 84.4±76.2% reduction.

The correlation analysis between tourist numbers and in situ nutrient concentrations (Table 4) showed distinct patterns between the two periods. During the pre-COVID-19 period, tourist numbers exhibited statistically significant positive correlations ($p<0.05$) with both PO_4^{3-}-P and NH_4^+-N concentrations across all environments (surface water, bottom water, and sediment).

For NH_4^+-N, the correlations were strongest in bottom water, followed by surface water, and weakest in sediment. For PO_4^{3-}-P, however, the correlation strengths in surface water and bottom water were very similar and both were considerably stronger than in sediment.

In contrast, no significant correlations were found during the COVID-19 period (all $p > 0.05$), likely due to dramatically reduced tourist numbers and the resulting alteration in anthropogenic nutrient input pathways and environmental dynamics.

Table 4. Correlation between tourist numbers and in situ nutrient concentrations (NH_4^+-N and PO_4^{3-}-P) in surface water, bottom water, and sediment (0–1 cm) during the pre-COVID-19 (2017–2019) and during-COVID-19 (2020–2021) periods, reported as the correlation coefficient (ρ) and p-value (significant set at $p<0.05$).

Correlation pair	Environment	Pre-COVID-19 (n = 70)		During-COVID-19 (n = 60)	
		ρ	p-value	ρ	p-value
Tourists vs. NH_4^+-N	Surface Water	0.577	0.032	0.249	0.349
	Bottom Water	0.587	0.021	-0.163	0.387
	Sediment (0-1 cm)	0.267	0.045	0.167	0.612
Tourists vs. PO_4^{3-}-P	Surface Water	0.589	0.028	-0.118	0.523
	Bottom Water	0.583	0.015	0.146	0.498
	Sediment (0-1 cm)	0.366	0.039	-0.166	0.678

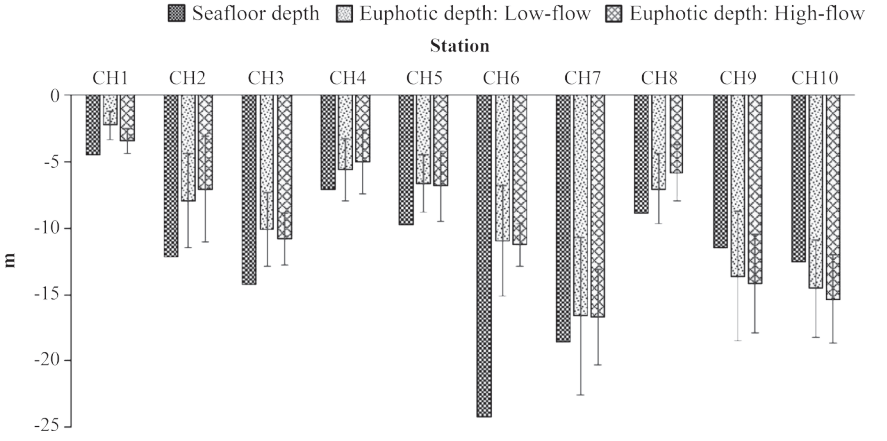

Figure 7. Comparison of seafloor depth and euphotic zone depth (m) at stations CH1–CH10 between low-flow (December–May) and high-flow (June–November) periods. Euphotic zone depth was estimated from Secchi disk depth using a 1.84:1 ratio (Borowiak and Borowiak, 2016).

CONCLUSIONS

The study demonstrates that the COVID-19 pandemic lockdowns significantly improved coastal water and sediment quality in Chonburi Province, Thailand, by reducing anthropogenic pressures. Seasonal variation and runoff impacts revealed distinct hydrological patterns, with high-flow periods (June–November) driving sediment dynamics and nutrient transport, particularly near river mouths (stations CH1–CH5). Low-flow periods (December–May) had weaker effects on surface and bottom water quality in areas farther from the river (stations CH6–CH10). The lockdown measures stabilized environmental variability, allowing coastal ecosystems to revert to more natural seasonal patterns, as evidenced by reduced standard deviations in most water and sediment quality parameters.

Temporal comparisons between pre-COVID-19 (2017–2019) and during-COVID-19 (2020–2021) periods highlighted substantial improvements. Surface water transparency increased by 27%, while total suspended solids (TSS) and PO_4^{3-}-P concentrations decreased by 29% and 42%, respectively. Bottom water showed a 51% reduction in NO_2^-+NO_3^--N and a 43% decline in PO_4^{3-}-P. Sediment quality also improved, with decreases in AVS (10%), $Si(OH)_4$-Si (23%), and PO_4^{3-}-P (9%). However, the dramatic rise in Chl *a* concentrations (101% in surface water, 116% in bottom water) indicated enhanced phytoplankton productivity due to favorable light and nutrient conditions, particularly through sediment nutrient fluxes. These findings underscore the resilience of coastal ecosystems when anthropogenic pressures are reduced, though long-term recovery requires addressing legacy nutrient loads in sediments.

The study underscores the dual role of external (riverine) and local (tourism, industrial) pollution sources. The 84% reduction in tourist-derived nutrient discharges during lockdowns highlights tourism's significant impact on coastal water quality. While short-term improvements were evident, sustained management strategies targeting sediment nutrient reservoirs are crucial for long-term ecosystem recovery. These insights provide a foundation for policymakers to balance economic activities with environmental conservation in coastal zones.

ACKNOWLEDGEMENTS

This research was successfully conducted under the project "Development of Socio-Ecological Based Effective Fishery Management Policy for Good Governance in Sustainable Fishery of the Inner Gulf of Thailand," funded by the Agricultural Research Development Agency (Public Organization), and the project "Ocean Forecasts Modeling and Early Warning System for Gulf of Thailand: Phase 2 and 3 - Water Quality Modeling in the Upper Gulf of Thailand," supported by the Hydro-Informatics Institute (Public Organization). We extend our sincere gratitude to the Department of Marine Science, Faculty of Fisheries, Kasetsart University, for providing laboratory facilities and research space. Special thanks to all faculty members of the Faculty of Fisheries, Kasetsart University, for their invaluable guidance and support throughout this research.

LITERATURE CITED

Allen, H.E. and G. Fu and B. Deng. 1993. Analysis of acid volatile sulfide (AVS) and simultaneously extracted metals (SEM) for sediment toxicity evaluations. **Environmental Toxicology and Chemistry** 12(8): 1441–1453. DOI: 10.1002/etc.5620120812.

ASTM. 2017. **Standard Test Methods for Particle-Size Distribution (Gradation) of Soils Using Sieve Analysis (ASTM D6913-17).** ASTM International, West Conshohocken, PA, USA. 34 pp. DOI: 10.1520/D6913_D6913M-17.

Bengtsson, L. and M. Enell. 1986. **Chemical analysis.** In: Handbook of Holocene Palaeoecology and Palaeohydrology (ed. B.E. Berglund), pp. 423–451. John Wiley and Sons Ldt., Chichester, UK.

Bianchi, T.S., M.A. Allison and W.J. Cai. 2013. **Biogeochemical Dynamics at Major River-Coastal Interfaces: Linkages with Global Change.** Cambridge University Press, Cambridge, UK. 694 pp.

Borowiak, D. and M. Borowiak. 2016. Comparative studies of underwater light regimes in lakes of the East Suwalki Lakeland. **Limnological Review** 16(4): 173–183. DOI: 10.1515/limre-2016-0019.

Breusch, T.S. and A.R. Pagan. 1979. A simple test for heteroscedasticity. **Econometrica** 47(5): 1287–1294. DOI: 10.2307/1911963.

Chakraborty, S., A. Mitra, P. Pramanick, S. Zaman and A. Mitra. 2020. Scanning the water quality of lower gangetic delta during COVID-19 lockdown phase using dissolved oxygen (DO) as proxy. **NUJS Journal of Regulatory Studies** 5: 69–74. DOI: 10.2139/ssrn.3663937.

Cherif, E.K., M. Vodopivec, N. Mejjad, J.C.G. Esteves da Silvan, S. Simonovic and H. Boulaassal. 2020. COVID-19 pandemic consequences on coastal water quality using WST Sentinel-3 data: Case of Tangier, Morocco. **Water** 12: 2638 DOI: 10.3390/w12092638.

Conley, D.J., H.W. Paerl, R.W. Howarth, D.F. Boesch, S.P. Seitzinger, K.E. Havens, C. Lancelot and G.E. Likens. 2009. Controlling eutrophication: Nitrogen and phosphorus. **Science** 323: 1014–1015. DOI: 10.1126/science.1167755.

Dean, W.E. 1974. Determination of carbonate and organic matter in calcareous sediments and sedimentary rocks by loss on ignition: Comparison with other methods. **Journal of Sedimentary Petrology** 44(1): 242–248. DOI: 10.1306/74D729D2-2B21-11D7-8648000102C1865D.

Department of Marine and Coastal Resources. 2018. **Marine and coastal resources information, Chonburi Province.** https://inter.fisheries.go.th/eng/en_pic/20211016213724 1_file.pdf. Cited 15 Jul 2025.

Dodds, W.K. and M.R. Whiles 2010. **Freshwater Ecology: Concepts and Environmental Applications.** Academic Press, London, UK. 811 pp.

Doney, S.C., V.J. Fabry, R.A. Feely and J.A. Kleypas. 2009. Ocean acidification: The other CO_2 problem. **Annual Review of Marine Science** 1: 169–192. DOI: 10.1146/annurev.marine.010908.163834.

Eastern Regional Irrigation Hydrology Center. 2023. **Runoff statistics 1995-2022.** Office of Water Management and Hydrology, Royal Irrigation Department. https://water.rid.go.th/hyd/PORTAL/monthly/basin_10.pdf. Cited 11 Mar 2025.

Faculty of Fisheries. 2018. **Development of Socio-Ecological Based Effective Fishery Management Policy for Good Governance in Sustainable Fishery of the Inner Gulf of Thailand.** Faculty of Fisheries, Kasetsart University, Bangkok, Thailand. 741 pp.

Gastec Corporation. 2023. **Detector tube handbook (Rev. 12).** Gastec Co., Ltd. Japan. https://www.gastec.co.jp. Cited 15 Jun 2023.

Gautam, S. 2020. The influence of COVID-19 on air quality in India: A boon or inutile. **Bulletin of Environment Contamination and Toxicology** 104(6): 724–726. DOI: 10.1007/s00128-020-02877-y.

Ignatiades, L., M. Karydis and P. Vounatsou. 1992. A possible method for evaluating oligotrophy and eutrophication based on nutrient concentrations. **Marine Pollution Bulletin** 24(5): 238–243. DOI: 10.1016/0025-326X(92)90561-J.

Imai, I., M. Yamaguchi and Y. Hori. 2006. Eutrophication and occurrences of harmful algal blooms in the Seto Inland Sea, Japan. **Plankton and Benthos Research** 1(2): 71–84. DOI: 10.3800/pbr.1.71.

Karydis, M. 2005. Understanding marine eutrophication from agriculture runoff in semi enclosed areas: a presentation of quantitative methodology. **Global NEST Journal** 7(2): 228–235.

Kutner, M.H., C.J. Nachtsheim, J. Neter and W. Li. 2005. **Applied Linear Statistical Models,** 5th ed. McGraw-Hill, Irwin, New York, USA. 1396 pp.

Lal, P., A. Kumar, S. Kumar, S. Kumari, P. Saikia, A. Dayanandan, D Adhikari and M.L. Khan. 2020. The dark cloud with a silver lining: Assessing the impact of the SARS COVID-19 pandemic on the global environment. **Science of the Total Environment** 732: 139297. DOI: 10.1016/j.scitotenv.2020.139297.

Loh, H.C., I. Looi, A.S.H. Ch'ng, K.W. Goh, L.C. Ming and K.H. Ang. 2022. Positive global environmental impacts of the COVID-19 pandemic lockdown: A review. **GeoJournal** 87: 4425–4437. DOI: 10.1007/s10708-021-10475-6.

Mallik, A., P. Chakraborty, S. Bhushan and B.B. Nayak. 2022. Impact of COVID-19 lockdown on aquatic environment and fishing community: Boon or bane?. **Marine Policy** 141: 105088. DOI: 10.1016/j.marpol.2022.105088.

Meksumpun, S. 2015. **Physiology and Ecology of Marine Phytoplankton.** Faculty of Fisheries, Kasetsart University, Bangkok, Thailand. 419 pp.

Ministry of Public Health. 2021. **Situation of coronavirus disease 2019 (COVID-19) public health measures and obstacles in disease prevention and control in travelers.** https://ddc.moph.go.th/uploads/files/2017420210820025238.pdf. Cited 19 Jun 2025.

Ministry of Tourism and Sports. 2025. **Domestic tourism statistics 2017–2021.** https://www.mots.go.th/more_news_new.php?cid=411. Cited 30 Jun 2025.

Mishra, A.K., A. Mishra, S.K. Mohakud, P. Acharya, P.R. Muduli and S.H. Farooq. 2024. COVID-19 induced lockdown reduced metal concentration in the surface water and bottom sediment of Asia's largest lagoon, **Marine Pollution Bulletin** 209(A): 117127. DOI: 10.1016/j.marpolbul.2024.117127.

Parsons, T.R., Y. Maita and C.M. Lalli. 1984. **A Manual of Chemical and Biological Methods for Seawater Analysis.** Pergamon Press Japan, Tokyo, Japan. 173 pp.

Pollution Control Department. 2005. **Study on Pollution Carrying Capacity of Koh Chang Area. Pollution Control Department, Ministry of Natural Resources and Environment.** Pollution Control Department, Bangkok, Thailand. 467 pp.

Regnier, P., S. Arndt, N. Goossens, C. Volta, G.G. Laruelle, R. Lauerwald and J. Hartmann. 2013. Modelling estuarine biogeochemical dynamics: From the local to the global scale. **Aquatic Geochemistry** 19: 591–626. DOI: 10.1007/s10498-013-9218-3.

Seitzinger, S.P., E. Mayorga, A.F. Bouwman, *et al*. 2010. Global river nutrient export: A scenario analysis of past and future trends. **Global Biogeochemical Cycles** 24(4): GB0A08. DOI: 10.1029/2009GB003587.

Shapiro, S.S. and M.B. Wilk. 1965. An analysis of variance test for normality. **Biometrika** 52(3–4): 591–611. DOI: 10.2307/2333709.

Sinutok, S., P. Chotikarn and M. Yucharoen. 2021. Impact of Covid-19 on coastal environment and activities at Ko Yo, Songkhla, Thailand. **Applied Ecology and Environmental Research** 19(4): 2815–2828. DOI: 10.15666/aeer/1904_28152828.

Thai Meteorological Department (TMD). 2016. **Climate of Thailand.** Thai Meteorological Department, Thailand. http://www.tmd.go.th/en/archive/season.php. Cited 25 Jun 2016.

Tokatlı, C. and M. Varol. 2021. Impact of the COVID-19 lockdown period on surface water quality in the Meriç-Ergene River Basin, Northwest Turkey. **Environmental Research** 197: 111051. DOI: 10.1016/j.envres.2021.111051.

Verardo, D.J., A. McIntyre and P.N. Froelich. 1990. Determination of organic carbon and nitrogen in marine sediments using the Carlo Erba NA-1500 analyze. **Deep Sea Research Part A, Oceanographic Research Papers** 37(1): 157–165. DOI: 10.1016/0198-0149(90)90034-S.

Virkanen, J., A. Korhola, M. Tikkanen and T. Blom. 1997. Recent environmental changes in a naturally acidic rocky lake in southern Finland, as reflected in its sediment geochemistry and biostratigraphy. **Journal of Paleolimnology** 17(2): 191–213. DOI: 10.1023/A:1007919922330.

World Health Organization. 2020a. **Infection prevention and control during health care when novel coronavirus (nCoV) infection is suspected: interim guidance.** https://www.who.int/publications/i/item/10665-331495. Cited 25 Jan 2025.

World Health Organization. 2020b. **Novel coronavirus (VoCn-2019), situation report 3, 23 January 2020.** https://www.who.int/docs/default-source/coronaviruse/situation-reports/20200123-sitrep-3-2019-ncov.pdf. Cited 10 Mar 2025.

Xu, H., G. Xu, X. Wen, X. Hu and Y. Wang. 2021. Lockdown effects on total suspended solids concentrations in the Lower Min River (China) during COVID-19 using time-series remote sensing images. **International Journal of Applied Earth Observation and Geoinformation** 98: 102301. DOI: 10.1016/j.jag.2021.102301.

Yan, H., H. Zhang and J.J. Huang. 2025. Quantifying coastal water quality responses to pandemic-induced human mobility: Insights from Bohai Bay. **Water Research** 285: 124043. DOI: 10.1016/j.watres.2025.124043.

Zambrano-Monserrate, M.A., M.A. Ruano and L. Sanchez-Alcalde. 2020. Indirect effects of COVID-19 on the environment. **Science of The Total Environment** 728: 138813. DOI: 10.1016/j.scitotenv.2020.138813.

Zhu, N., D. Zhang, W. Wang, et al. 2020. A novel coronavirus from patients with pneumonia in China, 2019. **The New England Journal of Medicine** 382(8): 727–733. DOI: 10.1056/NEJMoa2001017.